ARTICLE

Switchable Surfaces Based on Freely Floating Colloidal Particles

Nikolay Puretskiy, Georgi Stoychev, Manfred Stamm, and Leonid Ionov*

Leibniz Institute of Polymer Research Dresden, Hohe Strasse 6, D-01069 Dresden, Germany

ABSTRACT We report a novel approach for the design of switchable surfaces using hydrophobic wax films with incorporated hydrophilic particles. It was found that native and 3-aminopropyltriethoxysilane-modified 200 nm large silica particles almost completely immerse in wax after annealing in dry environment above wax melting point. On the other hand, the degree of particles immersion in wax decreases after annealing in aqueous environment. The surface properties of the particle-wax films are, therefore, switched between hydrophobic and hydrophilic states after annealing in air and in water, respectively. The hydrophilicity/hydrophibicity can be frozen by the cooling below the wax melting point. We also demonstrated possibility to produce hydrophilic/hydrophobic pattern on wax-particle films using local heating.

KEYWORDS: particles • wax • interfaces • switchable surfaces • patterning, wetting

INTRODUCTION

Surfaces with switchable/adaptive behavior (1−8) are of growing interest for the design of microfluidic devices (9−11), sensors (12−15), functional coatings (16−19), logical devices (20), and for biotechnological applications (21−25). To date, stimuli-responsive surface were designed mainly using self-assembled monolayers, polymer brushes (26), or using metal oxides (27). Exposure to environmental stimuli (solvent, pH, temperature, and light) of these materials changes composition in the topmost layer that affects their surface properties including adhesion, friction and wetting.

Recently, it was found that switching range of wetting properties of stimuli-responsive surfaces could be dramatically increased using rough substrates. According to equations of Wenzel (28−30) and Cassie (29, 31), roughness "enhances" intrinsic wetting properties of materials and makes hydrophilic/hydrophobic materials even more hydrophilic/hydrophobic, respectively. Using this principle, Minko et al., for example, fabricated mixed hydrophobic−hydrophilic brushes grafted to rough substrates, which demonstrate very broad switching range between absolute wetting (water contact angle is close to 0°) and ultrahydrophobicity (water contact angle is more then 150°) (17). On the other hand, surface roughness and therefore wetting properties of composite hydrogels can be switched by deformation (18).

Here we suggest a novel approach for the design of surfaces where both chemical composition and roughness can be switched by external stimuli. The approach is based on use of hydrophilic particles deposited on a surface of hydrophobic oil, whose melting point is slightly higher than the ambient temperature (e.g., wax). The degree of particle immersion in the molten wax layer is determined by the interfacial forces, which depend on environment - dry or aqueous. Therefore, roughness as well as hydrophobicity/hydrophilicity of the particle-wax surface can be reversibly switched by applying dry and aqueous media. Moreover, obtained morphologies can be "frozen" by cooling down below wax melting point.

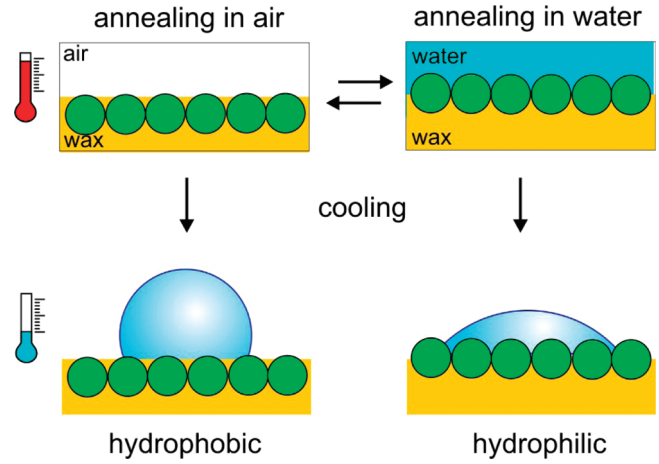

FIGURE 1. Scheme of switching of wax-particle surfaces. The hydrophilic particles are mixed with wax. Annealing in water and in air changes depth of immersion of the particles in oil layer that switches properties of the layer between hydrophilic and hydrophobic states.

EXPERIMENTAL SECTION

Preparation of Silica Particles. Silica particles (200 nm) were prepared by two-step synthesis according procedure described in ref 32. In brief, 1.5 mL of tetraethyl orthosilicate (TEOS) was added to a mixture of 50 mL of ethanol and 3 mL of saturated ammonia solution (28−30%) was added 1.5 mL tetraethyl orthosilicate (TEOS). The solution was mixed by magnetic stirrer (700 rpm) for 18 h. Resulting suspension was used for a further growth reaction. In second step, in a mixture of 25 mL of the suspension, 175 mL of ethanol, and 12 mL of ammonia (28 − 30%) was added 6 mL of TEOS. The solution was stirred (800 rpm) for 24 h. Particles were centrifuged and then rinsed with

* Corresponding author. E-mail: ionov@ipfdd.de.
Received for review July 20, 2010 and accepted September 14, 2010

DOI: 10.1021/am100634m

Published on Web 10/04/2010

ethanol several times followed by drying under a vacuum at 60 °C (2 h). The size of the silica particles and the polydispersity were controlled by SEM after each of the steps (ca. 100 nm after the first step, ca. 200 nm after the second step).

Modification of Silica Particles by 3-Aminopropyltriethoxysilane (APS). Dry silica particles (0,2 g) were added to a solution 0.8 mL of APS in 5 mL of ethanol for 3 h. To remove unreacted APS the particles were rinsed and centrifuged five times in ethanol. Finally, APS modified silica particles were dried under vacuum at 60 °C (2 h).

Preparation of Colloidosomes and Wax-Particle Films. The colloidosomes were prepared by following procedure. Native or APS-modified particles (100 mg) were dispersed in chloroform (10 mL) at room temperature. Then paraffin wax (2 g, mp 58 − 62 °C) were added, the system was heated up to 60 °C and sonicated 15 min. Hot water (40 mL) was added after evaporation of chloroform. Mixture was stirred and after 30 min rapidly cooled. Colloidosomes were filtered out and dried in the vacuum oven (40 °C, 15 mbar) during 12 h. Wax-particle films were prepared by melting of colloidosomes on the surface of water.

Scanning Electron (SEM) and Atomic force (AFM) Microscopy. All SEM micrographs were acquired on an environmental scanning electron microscope (ESEM, Philips XL-30), (DSM 982 Gemini, ZEISS, Germany) operating at 50 kV in the secondary electron (SE) mode. AFM studies were performed with a Dimension 3100 (Digital Instruments, Inc., Santa Barbara, CA) microscope. Tapping mode was used to map the film morphology at ambient conditions.

Contact Angle Measurements. Advancing and receding water contact angles were measured by the sessile drop method using a conventional drop shape analysis technique (Krüss DSA 10, Hamburg, Germany). Deionized reagent grade water was used for contact angle measurements. Liquid droplets (10-μL) were dropped carefully onto the sample surface, and the average value of 5 measurements, made at different positions of the same sample, was adopted as the average values of contact angles of the substrates. The error of the mean contact angle values, calculated as the standard deviation, did not exceed 2 and 3°. All contact angle measurements were carried out at 24 ± 0.5 °C and relative humidity of 40 ± 3%, which were kept constant.

RESULTS AND DISCUSSIONS

In our work, we investigated behavior of native and 3-aminopropyltriethoxysilane (APS)-modified 200 nm large silica particles on the wax surface. First, we tested the effect of gravity. We melted wax-native silica particle colloidosomes, which were prepares as described in ref 33, on the upper surface of horizontally positioned silica wafer as well as on a similar wafer, which was turned over. The particles were almost completely immersed in wax in both cases as it was revealed by AFM (results are not shown). Therefore, we conclude that gravity does not influence the degree of particle immersion in wax. In agreement with experimental results, theoretical calculations predict that interfacial forces acting on 200 nm large particles are on the order of 1×10^{-10} N that dramatically exceed the gravity force, which is estimated to be in order of 1×10^{-19} N.

Second, we investigated behavior silica particle on the surface of wax in aqueous and dry environment. The films were prepared by melting of wax-particle colloidosomes on the water surface. One side (upper one) is therefore annealed in dry conditions and another side (lower one) is annealed in aqueous environment. We found that both native and

Table 1. Experimentally Measured Values of Contact Angles at Different Flat Interfaces

interface	water contact angle (deg)	interface	hexadecane contact angle (deg)
APS−water−air	70	SiO_2−hexadecane−water	0
SiO_2−water−air	43	SiO−hexadecane−water	154
wax−water−air	107	APS−hexadecane−air	0
		APS−hexadecane−water	122

APS-modified silica particles almost completely immersed into wax at the wax-air interface. On the other hand, both sorts of particles were found to be only slightly immersed in wax at the water-wax interface. The height of the particle cap above the wax surface normalized to the particle radius (h^*) is slightly different, $h^* = 1.3$ and $h^* = 1.1$, respectively. This ratio is in good qualitative correlation with previously obtained results (33) as well as with our estimation based on contact angle data (Table 1) using formula $h^* = 1 - \cos \Theta_{wax}^{air\_or\_water}$ (34). The quantitative difference between experimental and predicated values can be explained by the intrinsic roughness of the particles and the difference between advancing and receding contact angles of wax on particle surface.

Next, we theoretically and experimentally investigated wetting properties of composite wax-particle surfaces. The wetting properties of these surfaces are determined by several parameters: hydrophilicity and surface roughness provided by particles as well as hydrophobicity of wax. Although there are many models, which may be used to simulate wetting behavior of wax surfaces with particles, we applied the Cassie−Baxter equation, eq 1. This choice is justified by our recent experimental findings where we demonstrated that the Cassie−Baxter equation provides the best agreement with the experimental results for wetting behavior on surfaces made of colloidal particles (34−36). For simplicity, we considered only the case when the water droplets collapsed on the surface. In this case, liquid completely fills the grooves between particle-collapsed drop. The following modification of the Cassie−Baxter equation was used

$$\cos \Theta = f_{particle}^{wax} r_{particle}^{wax} \cos \Theta_{particle}^{water} + (1 - f_{particle}^{wax}) \cos \Theta_{wax}^{water} \quad (1)$$

where $\cos \Theta_{particle}^{water}$ and $\cos \Theta_{wax}^{water}$ are the intrinsic water contact angles on the surfaces of particles and wax (Table 1, left column), respectively; $f_{particle}^{wax} = n\pi R_p^2(2h^* - h^{*2})$ is the area fraction of particles on the surface of wax; $r_{particle}^{wax} = (2)/(2 - h^*)$ is roughness factor of particle cap above wax surface; h^* is normalized height of particle cap above wax surface (Table 2, experimental values); $\Theta_{wax}^{air\_or\_water}$ is intrinsic contact angle of wax on the particle surface in air or aqueous environment (Table 1, right column); $n = (N)/(S)$ is the number of particles (N) per areas (S); $n_{max} = (1)/(2\sqrt{3}R_p^2)$ is maximum number density of particles on surface, which corresponds to closely packed particles. Performed simula-

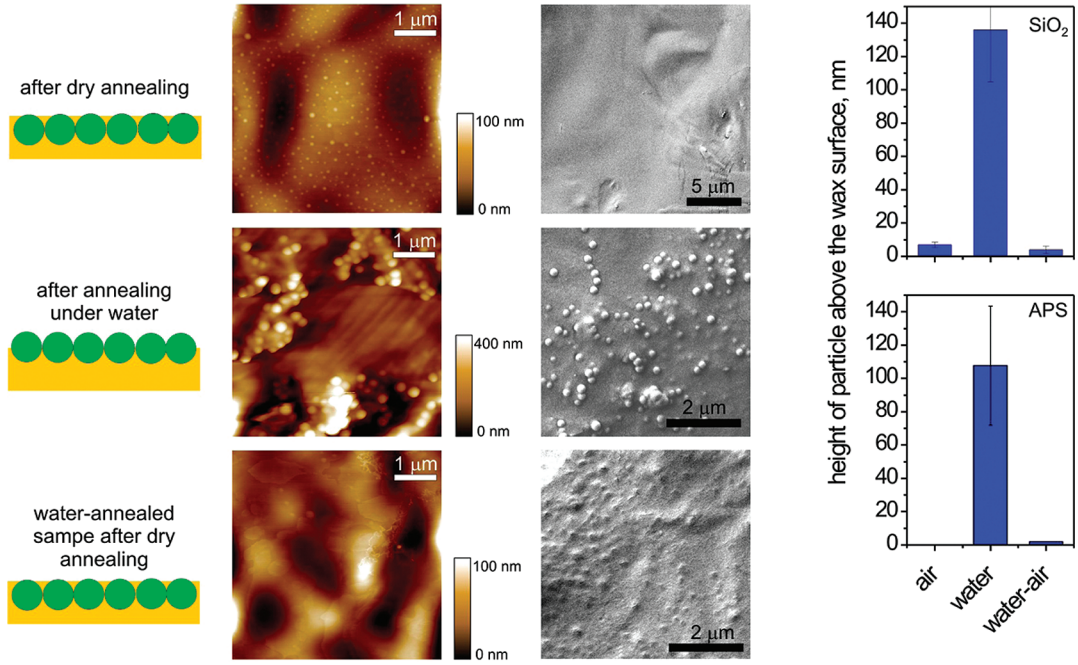

FIGURE 2. Immersion of native silica particles into wax surface after annealing in air (upper panel), annealing in water (middle panel) and annealing in air of the sample, which was preliminary annealed in water (lower panel). AFM (second from left column) and SEM (third from left column) images of silica particles on wax surface. Height of the particle cap above wax surface after annealing in air, in water, and after second annealing in air of native and APS-modified silica particles derived from AFM images (right plots).

Table 2. Experimentally Obtained and Estimated Degree of Immersion of Unmodified and APS-Modified Silica Particles in Wax Depending on Environment

		height of the particle cap above the wax surface normalized to the particle radius, h^*		
particles	annealing conditions	experimental	experimental from ref 33	estimated using contact angles from Table *1*
native	air	0.1		0
	water	1.3	1.8	1.9
APS-modified	air	0		0
	water	1.1	1.5	1.54

tions demonstrate that the native and APS-modified particle-wax surfaces provide different wetting properties after annealing on air and in water, and that the particle-wax surface is hydrophilic after annealing in water and is hydrophobic after annealing in air. The contrast between hydrophilic and hydrophobic states increases with the density of particles on the surface (Figure 3a).

Experimental investigation of the wetting properties on obtained wax-particle layers after annealing in different media was performed using water contact angle measure-

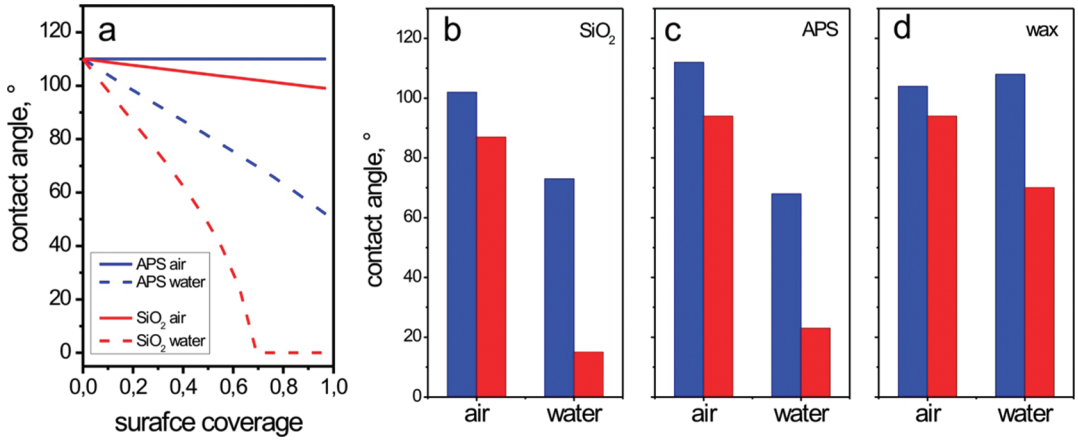

FIGURE 3. (a) Simulated and (b−d) experimentally obtained wetting properties of particle-wax surfaces after annealing in dry and aqueous environment. (a) Simulated water contact angle on native (red lines) and APS-modified (blue lines) wax-particle surfaces after annealing in air (solid lines) and in water (dashed lines) at different surface coverage of wax surface by the particles. Water advancing (blue) and receding (red) contact angles after annealing in air and in water of (b) wax-silica particle surface; (c) wax-APS-modified silica particle surface; (d) reference wax surface.

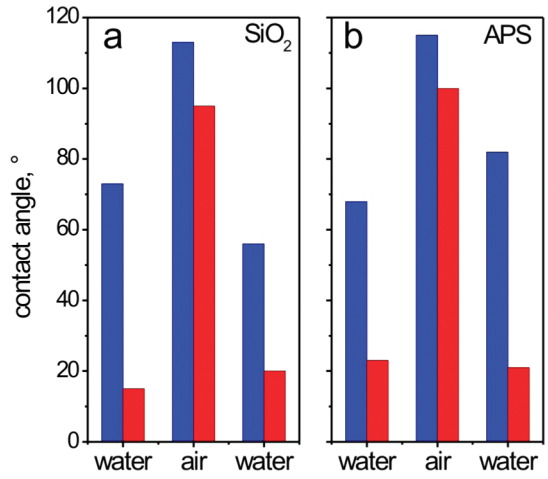

FIGURE 4. Switching of advancing (blue) and receding (red) water contact angles on (a) wax-silica particle and (b) wax-APS particle surfaces after sequential annealing in water, in air, and in water again.

ments. We measured both advancing (Θ_{adv}) and receding (Θ_{rec}) water contact angles. We found that the wax-particle surfaces are more hydrophilic after annealing in water ($\Theta_{adv} = 60-70°$, $\Theta_{rec} = 10-20°$) then after annealing in air ($\Theta_{adv} = 100-110°$, $\Theta_{rec} = 90-95°$, Figure 3b,c). Because of small contact angle hysteresis, the water droplets are flexible on the wax-particle surface annealed in air and can be removed by slight shaking. On the other hand, the water droplets remain strongly pinned to the wax-particle surface after annealing in water. We performed a control experiment and investigated wetting properties of wax without particles annealed on air and in water. The wax surface becomes slightly more hydrophilic after annealing in aqueous environment, which is seen from the decrease of the receding contact angle: $\Theta_{rec} = 90°$ and $\Theta_{rec} = 70°$ after annealing in air and in water, respectively (Figure 3d). The advancing water contact angles on the wax surfaces annealed in dry and aqueous environment are nearly the same: $\Theta_{adv} = 100-105°$. Therefore, we can conclude that the difference in wetting properties of wax-particle surface annealed at different conditions originates from the different degrees of immersion of particles into wax surface.

We experimentally tested the possibility of reversibly switching wetting properties of the particle-wax surfaces. The hydrophilic wax-particle film, which was preliminary annealed in water, was used for the switching experiments. This film was then melted in dry state. We found that the particle-wax film switches into hydrophobic state after annealing in air (Figure 4). The second annealing in water switches the surface back into the hydrophilic state (Figure 4). Further annealing in air and in water switches the layer in hydrophilic and hydrophobic states, respectively. Thus, the wax-particle layer demonstrates the fully reversible switching of wetting properties after annealing in dry and aqueous environment.

Finally, we demonstrated applicability of the developed stimuli-responsive surfaces for hydrophilic–hydrophobic patterning. We used the particle-wax film, which was preliminary switched to hydrophilic state by annealing in water,

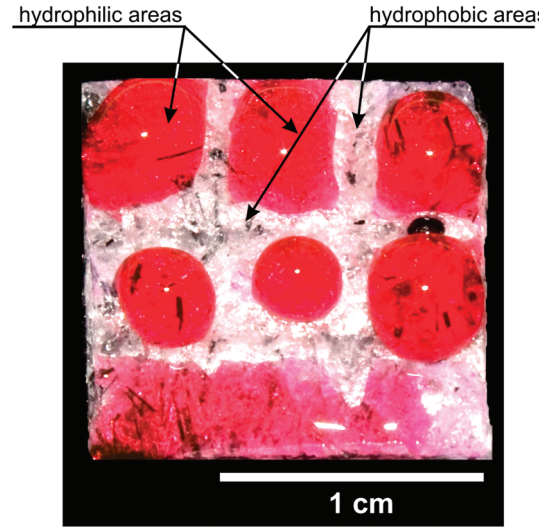

FIGURE 5. Hydrophilic/hydrophobic patterning of APS-particle/wax surface using heated needle. APS-particle/wax surface was switched to hydrophilic state by annealing in aqueous environment. Applying heated needle locally switches the surface into hydrophobic state. Water (colored with rhodamine) selectively wets the hydrophilic areas and is unable to wet the areas where the needle was applied (white areas marked as hydrophobic).

and locally applied heat using a hot needle. The needle was brought in the proximity to the surface with no direct contact between them. As expected, the particle-wax surface locally switches in hydrophobic state. In fact, we found that water readily wets areas where no needle was applied (hydrophilic areas), whereas water does not wet the areas where the needle was applied (hydrophobic area). In this way, we can write a structure into a sample surface.

CONCLUSIONS

We developed a novel approach for design of stimuli-responsive surfaces. The approach is based on hydrophobic waxy surfaces with incorporated hydrophilic particles. The degree of particle immersion in liquid oil layer was demonstrated to depend on environment (dry or aqueous). Thus, roughness as well as hydrophobicity/hydrophilicity of the particle-wax surface can be switched in dry and aqueous environments as well as can be frozen by cooling down below melting point of wax. We also demonstrated the possibility to pattern wax-particle surfaces using locally applied heat, for instance warm needle. Moreover, we propose that the patterning can also be performed using localized heating by laser beam. The developed approach can find a broad application for design of switchable surfaces for offset printing of pigments, proteins as well as cells.

Acknowledgment. This work was supported by the DFG (grant IO 68/1-1), VW Foundation and the Leibniz Institute of Polymer Research Dresden.

REFERENCES AND NOTES

(1) Winnik, F. M.; Whitten, D. G.; Urban, M. W. *Langmuir* **2007**, *23*, 1–2.
(2) Luzinov, I.; Minko, S.; Tsukruk, V. V. *Prog. Polym. Sci.* **2004**, *29*, 635–698.
(3) Cole, M. A.; Voelcker, N. H.; Thissen, H.; Griesser, H. J. *Biomaterials* **2009**, *30*, 1827–1850.

(4) Tokarev, I.; Minko, S. *Soft Matter* **2009**, *5*, 511–524.
(5) Sun, A.; Lahann, J. *Soft Matter* **2009**, *5*, 1555–1561.
(6) Mendes, P. M. *Chem. Soc. Rev.* **2008**, *37*, 2512–2529.
(7) Luzinov, I.; Minko, S.; Tsukruk, V. V. *Soft Matter* **2008**, *4*, 714–725.
(8) Stuart, M. A. C.; Huck, W. T. S.; Genzer, J.; Muller, M.; Ober, C.; Stamm, M.; Sukhorukov, G. B.; Szleifer, I.; Tsukruk, V. V.; Urban, M.; Winnik, F.; Zauscher, S.; Luzinov, I.; Minko, S. *Nat. Mater.* **2010**, *9*, 101–113.
(9) Synytska, A.; Stamm, M.; Diez, S.; Ionov, L. *Langmuir* **2007**, *23*, 5205–5209.
(10) Ionov, L.; Houbenov, N.; Sidorenko, A.; Stamm, M.; Luzinov, I.; Minko, S. *Langmuir* **2004**, *20*, 9916–9919.
(11) Ionov, L.; Houbenov, N.; Sidorenko, A.; Stamm, M.; Minko, S. *Adv. Funct. Mater.* **2006**, *16*, 1153–1160.
(12) Tagit, O.; Tomczak, N.; Benetti, E. M.; Cesa, Y.; Blum, C.; Subramaniam, V.; Herek, J. L.; Vancso, G. J. *Nanotechnology* **2009**, *20*, 185501.
(13) Ionov, L.; Minko, S.; Stamm, M.; Gohy, J. F.; Jerome, R.; Scholl, A. *J. Am. Chem. Soc.* **2003**, *125*, 8302–8306.
(14) Ionov, L.; Sapra, S.; Synytska, A.; Rogach, A. L.; Stamm, M.; Diez, S. *Adv. Mater.* **2006**, *18*, 1453–1457.
(15) Tokareva, I.; Minko, S.; Fendler, J. H.; Hutter, E. *J. Am. Chem. Soc.* **2004**, *126*, 15950–15951.
(16) Sidorenko, A.; Minko, S.; Schenk-Meuser, K.; Duschner, H.; Stamm, M. *Langmuir* **1999**, *15*, 8349–8355.
(17) Minko, S.; Muller, M.; Motornov, M.; Nitschke, M.; Grundke, K.; Stamm, M. *J. Am. Chem. Soc.* **2003**, *125*, 3896–3900.
(18) Sidorenko, A.; Krupenkin, T.; Taylor, A.; Fratzl, P.; Aizenberg, J. *Science* **2007**, *315*, 487–490.
(19) Lahann, J.; Mitragotri, S.; Tran, T. N.; Kaido, H.; Sundaram, J.; Choi, I. S.; Hoffer, S.; Somorjai, G. A.; Langer, R. *Science* **2003**, *299*, 371–374.
(20) Motornov, M.; Zhou, J.; Pita, M.; Gopishetty, V.; Tokarev, I.; Katz, E.; Minko, S. *Nano Lett.* **2008**, *8*, 2993–2997.
(21) Alarcon, C. D. H.; Pennadam, S.; Alexander, C. *Chem. Soc. Rev.* **2005**, *34*, 276–285.
(22) Ionov, L.; Stamm, M.; Diez, S. *Nano Lett.* **2006**, *6*, 1982–1987.
(23) Yamada, N.; Okano, T.; Sakai, H.; Karikusa, F.; Sawasaki, Y.; Sakurai, Y. *Makromol. Chem., Rapid Commun.* **1990**, *11*, 571–576.
(24) Huber, D. L.; Manginell, R. P.; Samara, M. A.; Kim, B. I.; Bunker, B. C. *Science* **2003**, *301*, 352–354.
(25) Ionov, L.; Synytska, A.; Diez, S. *Adv. Funct. Mater.* **2008**, *18*, 1501–1508.
(26) Senaratne, W.; Andruzzi, L.; Ober, C. K. *Biomacromolecules* **2005**, *6*, 2427–2448.
(27) Wang, R.; Hashimoto, K.; Fujishima, A.; Chikuni, M.; Kojima, E.; Kitamura, A.; Shimohigoshi, M.; Watanabe, T. *Nature* **1997**, *388*, 431–432.
(28) Wenzel, R. N. *Ind. Eng. Chem. Res.* **1936**, *28*, 988.
(29) Marmur, A. *Langmuir* **2003**, *19*, 8343–8348.
(30) Marmur, A. *Langmuir* **2004**, *20*, 3517–3519.
(31) Cassie, A. B. D.; Baxter, S. *Trans. Faraday Soc.* **1944**, *40*, 546–551.
(32) Nozawa, K.; Gailhanou, H.; Raison, L.; Panizza, P.; Ushiki, H.; Sellier, E.; Delville, J. P.; Delville, M. H. *Langmuir* **2005**, *21*, 1516–1523.
(33) Berger, S.; Synytska, A.; Ionov, L.; Eichhorn, K. J.; Stamm, M. *Macromolecules* **2008**, *41*, 9669–9676.
(34) Synytska, A.; Ionov, L.; Dutschk, V.; Stamm, M.; Grundke, K. *Langmuir* **2008**, *24*, 11895–11901.
(35) Synytska, A.; Ionov, L.; Grundke, K.; Stamm, M. *Langmuir* **2009**, *25*, 3132–3136.
(36) Synytska, A.; Ionov, L.; Dutschk, V.; Minko, S.; Eichhorn, K. J.; Stamm, M.; Grundke, K. *Prog. Colloid Polym. Sci.* **2006**, *132*, 72–81.

AM100634M